An X-ray investigation of the NGC 346 field in the SMC (1) : the LBV HD 5980 and the NGC 346 cluster

Y. Nazé[1]

Institut d'Astrophysique et de Géophysique, Université de Liège, Allée du 6 Août 17, Bat. B5c, B 4000 - Liège (Belgium)

naze@astro.ulg.ac.be

J.M. Hartwell and I.R. Stevens

School of Physics & Astronomy, University of Birmingham, Edgbaston, Birmingham B15 2TT (UK)

jmh@star.sr.bham.ac.uk, irs@star.sr.bham.ac.uk

M. F. Corcoran

Universities Space Research Association, High Energy Astrophysics Science Archive Research Center, Goddard Space Flight Center, Greenbelt, MD 20771 (USA)

corcoran@barnegat.gsfc.nasa.gov

Y.-H. Chu

Astronomy Department, University of Illinois, 1002 W. Green Street, Urbana, IL 61801 (USA)

chu@astro.uiuc.edu

G. Koenigsberger

Instituto de Astronomía, Universidad Nacional Autónoma de Mexico, Apdo. Postal 70-264, 04510, Mexico D.F. (Mexico)

gloria@astroscu.unam.mx

A.F.J. Moffat

Département de physique, Université de Montreal, C.P. 6128, Succ. Centre-Ville, Montreal, QC, H3C 3J7 (Canada)

moffat@astro.umontreal.ca

and

V.S. Niemela

Facultad de Ciencias Astronómicas y Geofísicas, Universidad Nacional de la Plata, Paseo del Bosque S/N, B19000FWA La Plata (Argentina)

virpi@fcaglp.fcaglp.unlp.edu.ar

ABSTRACT

We present results from a *Chandra* observation of the NGC 346 cluster. This cluster contains numerous massive stars and is responsible for the ionization of N66, the most luminous H II region and the largest star formation region in the SMC. In this first paper, we will focus on the characteristics of the main objects of the field. The NGC 346 cluster itself shows only relatively faint X-ray emission (with $L_X^{unabs} \sim 1.5 \times 10^{34}$ erg s^{-1}), tightly correlated with the core of the cluster. In the field also lies HD 5980, a LBV star in a binary (or possibly a triple system) that is detected for the first time at X-ray energies. The star is X-ray bright, with an unabsorbed luminosity of $L_X^{unabs} \sim 1.7 \times 10^{34}$ erg s^{-1}, but needs to be monitored further to investigate its X-ray variability over a complete 19 d orbital cycle. The high X-ray luminosity may be associated either with colliding winds in the binary system or with the 1994 eruption. HD 5980 is surrounded by a region of diffuse X-ray emission, which is a supernova remnant. While it may be only a chance alignment with HD 5980, such a spatial coincidence may indicate that the remnant is indeed related to this peculiar massive star.

Subject headings: (galaxies:) Magellanic Clouds–X-rays: individual (NGC 346, HD 5980)

1. Introduction

The Small Magellanic Cloud (SMC) is an irregular galaxy at a distance of 59 kpc (Mathewson, Ford, & Visvanathan 1986) that forms a pair with the Large Magellanic Cloud (LMC). Both are satellites of our own Galaxy. The interstellar extinction towards the

[1]Research Fellow F.N.R.S.

Magellanic Clouds is low, allowing studies of the X-ray sources to be undertaken with clarity.

Previous X-ray observations of the SMC have been made with the *Einstein Observatory*, *ASCA* and *ROSAT*. These observations included surveys of the point source population (Kahabka et al. 1999; Schmidtke et al. 1999; Haberl et al. 2000; Sasaki, Haberl, & Pietsch 2000; Yokogawa et al. 2000) and in particular studies of the properties of the X-ray binary population (Haberl & Sasaki 2000). The recent launch of *Chandra*, however, provides an opportunity to study the SMC with a far greater sensitivity and spatial resolution than ever before.

We have obtained a Chandra observation of the giant H II region N66 (Henize 1956), the largest star formation region in the SMC, in order to study the young cluster NGC 346 and its interaction with the surrounding interstellar medium. This cluster contains numerous massive stars (Massey, Parker & Garmany 1989), of spectral types as early as O2 (Walborn et al. 2002). The large number of massive stars is not the only feature of interest in this field. On the outskirts of NGC 346 lies the remarkable star HD 5980, which underwent a Luminous Blue Variable (LBV)-type eruption in 1994. This massive binary (or triple?) system has been monitored and analysed for its varying spectral and photometric properties in visible and UV wavelengths since the early 80's (Koenigsberger et al. 2000; Sterken & Breysacher 1997, and references therein). Previous X-ray observations of NGC 346 (Inoue, Koyama, & Tanaka 1983; Haberl et al. 2000) detected a bright extended source around HD 5980 which has been attributed to a supernova remnant (SNR); however, the crude instrumental resolution prohibited unambiguous detections of a point source associated with HD 5980. In addition to HD 5980, the young massive stars of NGC 346 and their interacting winds are likely to produce X-ray emission, but have not been detected previously. The sensitive, high-resolution *Chandra* observation of the NGC 346 field thus provides an excellent opportunity to study a variety of phenomena involving emission at X-ray energies.

In this paper, we will describe in § 2 the observations used in this study, then discuss the available data on NGC 346, HD 5980, and the extended emission in § 3, 4, and 5, respectively. Finally, conclusions are given in § 6. The second part of this work (Nazé et al., paper II) will describe the properties of the other sources detected in the field.

2. The Observations and Data Analysis

2.1. X-ray Observations

NGC 346 was observed with *Chandra* for the XMEGA[2] consortium on 2001 May 15–16 for 100 ks (98.671 ks effective, ObsID = 1881, JD∼2 452 045.2d). The data were recorded by the ACIS-I0, I1, I2, I3, S2 and S3 CCD chips maintained at a temperature of −120°C. The data were taken with a frame time of 3.241s in the faint mode. The exposure was centered on the cluster, with HD 5980 lying 1.9′ to the north-east of the aimpoint on ACIS-I3. Our faintest sources have fluxes of about 2×10^{32} erg s^{-1} (see paper II), assuming a distance of 59 kpc for the SMC.

We excluded bad pixels from the analysis, using the customary bad-pixel file provided by the *Chandra* X-ray Center (CXC) for this particular observation. We have searched the data for background flares, which are known to affect *Chandra* data, by examining the lightcurve of the total count rate, but no flares were found. Event Pulse Invariant (PI) values and photon energies were determined using the FITS Embedded File (FEF) acisD2000-01-29fef_piN0001.fits.

For long exposures, removing the afterglow events can adversely affect the science analysis (underestimation of the fluxes, alteration of the spectra and so on)[3]. We thus computed a new level 2 events file by filtering the level 1 file and keeping the events with *ASCA* grades of 0, 2, 3, 4 and 6, but without applying a status=0 filter. Throughout this paper, we will use this new file for all scientific analysis.

Further analysis was performed using the CIAO v2.1.2 software provided by the CXC and also with the FTOOLS tasks. The spectra were analysed and fitted within XSPEC v11.0.1 (Arnaud 1996). In Fig. 1, we show a 3 color image of the Chandra data of the NGC 346 cluster, HD 5980 and its surroundings. We will discuss the features of this image further in later sections.

We have investigated problems due to Charge Transfer Inefficiency (CTI). To remove these CTI effects, we used the algorithm of Townsley et al. (2000). Checking several sources

[2]http://lheawww.gsfc.nasa.gov/users/corcoran/xmega/xmega.html

[3]see caveat on http://asc.harvard.edu/ciao/caveats/acis_cray.html

on different chips and/or at different positions on each CCD, we concluded that the impact of the CTI was small and that it did not change significantly the spectral parameters found by using non-corrected data. When a difference was apparently found, we discovered that the best fits found on corrected and non-corrected data gave similar χ^2. As the work of Townsley et al. (2000)is not yet an official CXC product[4], we chose to present here only the results of the non-corrected data.

2.2. *HST* WFPC2 Images

Two *HST* WFPC2 observations of the N66 / NGC 346 region in Hα are available from the STScI archives. They were taken on 1998 Sept. 27 and 2000 August 7 for the programs 6540 and 8196, respectively. HD 5980 is centered on the PC in the observations from program 6540 (see Fig. 2), while program 8196 shows an area situated further south. The observations were made through the $F656N$ filter for 2070s (Prog. # 6540) and 2400s (Prog. # 8196). This filter, centered at 6563.7 Å with a FWHM of 21.4Å, includes the Hα line and the neighboring [N II] lines.

The calibrated WFPC2 images were produced by the standard *HST* pipeline. We processed them further with IRAF and STSDAS routines. The images of each program were combined to remove cosmic rays and to produce a total-exposure map. No obvious correlation between X-rays features and the Hα emission is seen in the *HST* data. Fig. 2 will be discussed more extensively in § 5.

3. The NGC 346 Star Cluster

The NGC 346 cluster has a large number of massive stars, containing almost 50% of all early-type O stars in the SMC (Massey, Parker & Garmany 1989). It is responsible for the ionization of N66, the most luminous H II region in the SMC (Ye, Turtle, & Kennicutt 1991). However, the NGC 346 cluster has not been detected in X-rays until this *Chandra* observation. Even though NGC 346 lies near the joint of the four ACIS-I CCD chips and part of the cluster is lost in the gaps between CCDs, the X-ray emission from the core of

[4]http://www.astro.psu.edu/users/townsley/cti/

NGC 346 is unambiguously detected in the corner of the ACIS-I3 chip. The X-ray emission appears extended with multiple peaks corresponding to the bright blue stars MPG 396, 417, 435, 470, and 476 (Fig. 3). As only ∼300 counts are detected and the X-ray peaks are not well-resolved, we will analyze only the overall emission from the cluster.

The total count rate of this emission in the $0.3 - 10.0$ keV band is $3.04 \pm 0.36 \times 10^{-3}$ cnts s^{-1}. The spectrum of the NGC 346 cluster was extracted from a square aperture of $\sim 45'' \times 45''$ with a carefully chosen background region, as close as possible to the cluster. As we regard the cluster X-ray emission to be extended, we have used the *calcrmf* and *calcarf* tools to generate the appropriate response files. The best fit (χ^2_ν=0.90, N_{dof}=50, $Z = 0.1 Z_\odot$) to this spectrum was an absorbed *mekal* model (Kaastra 1992) with the following properties (see Fig. 4): an absorption column density $N(H)$ of $0.42^{0.83}_{0.17} \times 10^{22}$ cm^{-2} and a temperature kT of $1.01^{2.23}_{0.61}$ keV. The luminosity in the $0.3 - 10.0$ keV band was 5.5×10^{33} erg s^{-1}, which corresponds to an unabsorbed luminosity of 1.5×10^{34} erg s^{-1}. The absorption column is comparable to the value expected for NGC 346 (see paper II), but the temperature is one of the lowest we found, except for the extended source around HD 5980.

In the region of X-ray emission in NGC 346, 30 blue stars were detected by Massey, Parker & Garmany (1989): MPG 435, 342, 470, 368, 476, 396, 487, 417, 370, 471, 467, 495, 451, 330, 455, 454, 500, 445, 468, 375, 508, 395, 439, 371, 485, 561, 374, 366, 557, 400 (by increasing magnitude). Of these, 16 have known spectral types that we can use to convert magnitudes to bolometric luminosities. The bolometric correction factors were taken from Humphreys & McElroy (1984). We can then compute the expected X-ray luminosities using $log(L_X^{unabs}) = 1.13 \log(L_{BOL}) - 11.89$ (Berghöfer et al. 1997). If the X-rays were coming only from these 16 stars, we should expect a total unabsorbed luminosity of 2×10^{33} erg s^{-1}. This represents only 13% of the detected luminosity. Several hypotheses could explain this discrepancy: a metallicity effect (Berghöfer's relation was determined for Galactic stars but SMC stars have weaker winds); X-ray emission from the other (unclassified) stars in this region, especially from the low-mass stars (see e.g. Getman et al. 2002); additional emission linked to interactions in binary systems (such as colliding winds); or an extended region of hot gas as the winds from the individual stars combine to form a cluster wind (Ozernoy, Genzel, & Usov 1997; Cantó, Raga, & Rodríguez 2000).

Chandra has also observed X-ray emission from other very young (age < 5 Myr) stellar clusters, comparable to NGC 346. The Arches cluster in the Galactic Center region has

been observed to have emission from several different regions, with a total X-ray luminosity of $L_X^{unabs} \sim 5 \times 10^{35}$ erg s^{-1} (Yusef-Zadeh et al. 2002). NGC 3603 has also been observed with *Chandra* (Moffat et al. 2002) and the total unabsorbed cluster luminosity is $L_X^{unabs} \sim 1 \times 10^{35}$ erg s^{-1} (though in this case it is clear that a substantial fraction of the emission is from point sources in the cluster). For both the Arches and NGC 3603 clusters the fitted temperature of the X-ray emission is higher than the $kT \sim 1$ keV value for NGC 346.

It is important to note that the calculations presented by Cantó, Raga, & Rodríguez (2000) and Raga et al. (2001) for the Arches cluster assume that there are about 60 stellar sources having mass-loss rates of 10^{-4} M$_\odot$ yr^{-1}. If we take the list of the bluest stars in NGC 346 given by Massey, Parker & Garmany (1989), the first 60 sources have spectral types in the range O3-B0. Assuming mass-loss rates for 8 SMC stars given by Puls et al. (1996) to be typical, then all stars in NGC 346 (excluding HD 5980) have mass-loss rates smaller than 10^{-4} M$_\odot$ yr^{-1}. Only MPG 435 (O4III(n)(f)) has a mass loss rate as high as 9×10^{-5} M$_\odot$ yr^{-1}. However, the majority of these 60 stars are late O-type Main Sequence stars or cooler, which must have much smaller mass-loss rates (10^{-6} M$_\odot$ yr^{-1} or less), and they are more widely distributed than in Arches. Thus, it is not surprising that the X-ray luminosity is lower than in Arches, and, in fact, it may be too large to be explained solely with the cluster wind scenario.

4. The LBV HD 5980

Among all stars in NGC 346, HD 5980 is unique in its spectral variations in the last two decades, and warrants further examination. This eclipsing binary (or triple system?) was classified as WN+OB before 1980, but its spectral type changed to WN3+WN4 in 1980–1983, and to WN6, with no trace of the companion in 1992. In 1994, this star underwent a LBV-type eruption, and presented at the same time a WN11 type. The eruption has now settled down and the spectrum is returning to its pre-eruption state (for more details see Koenigsberger et al. 2000, and references therein). We will label the 1994 eruptor as 'star A' and its companion as 'star B'.

Chandra is the first X-ray telescope to detect this peculiar system, since the low spatial resolution of previous X-ray observatories did not allow the distinction of HD 5980 from the extended emission surrounding it. However, even with a 100 ks exposure, the data possess a rather low signal-to-noise ratio. The *Chandra* ACIS-I count rate of HD 5980 is only $2.98 \pm 0.19 \times 10^{-3}$ cnts s^{-1} in the $0.3 - 10.0$ keV band or about 300 counts in the total ob-

servation. This limits our ability to sensitively determine the spectral shape of the emission and to look for source variability. On the other hand, the relative faintness of the source means that photon pileup will not affect our analysis to any great degree.

We have extracted a spectrum of HD 5980 using the CIAO tool *psextract*. An annular background region around the source (but sufficiently far from it) was chosen, in order to eliminate contamination from the surrounding extended emission (see § 5). This spectrum is shown in Fig. 5a. The best fit model to the spectrum has the following parameters: $N(H) = 0.22^{0.35}_{0.14} \times 10^{22}$ cm^{-2} and $kT = 7.04^{13.35}_{4.35}$ keV for an absorbed *mekal* model and $N(H) = 0.28^{0.44}_{0.19} \times 10^{22}$ cm^{-2} and Γ=$1.74^{1.89}_{1.53}$ for an absorbed power-law. These absorption columns are consistent with the value expected for NGC 346 (see paper II) but part of these columns are probably due to wind absorption and/or absorption from the 1994 ejecta. The derived observed X-ray luminosity of HD 5980 is $L_X = 1.3 \times 10^{34}$ erg s^{-1} in the $0.3 - 10.0$ keV band for both models. Using the normalisation factor of the *mekal* model, we found a volume emission measure of $\sim 10^{57}$ cm^{-3} for this source.

We can compare HD 5980 with other WR stars detected in X-rays. The unabsorbed X-ray luminosity of HD 5980 is 1.7×10^{34} erg s^{-1} in the $0.3 - 10.0$ keV energy range and 9×10^{33} erg s^{-1} in the *ROSAT* range, i.e. $0.2 - 2.4$ keV. This places HD 5980 amongst the X-ray brightest single WN stars (Wessolowski 1996) and the brightest WR+OB binaries (Pollock 2002) of the Galaxy.

Two factors could explain this high X-ray luminosity. First, the fast wind from the post-eruptive phases (from 1300 km s^{-1} in 1994 to $\sim$2000 km s^{-1} in 2000) should now collide with the slow wind (ejected with a velocity as low as 200 km s^{-1} during the eruption, see e.g. Koenigsberger et al. 2000), which will increase the post-eruptive X-ray luminosity. X-ray emission from colliding ejecta has already been observed for another LBV, i.e. η Carinae. An elliptically shaped extended emission of $40'' \times 70''$(i.e. 0.4 pc$\times$0.8 pc) in size surrounds the star in the X-ray domain (Seward et al. 2001). It is correlated to the high velocity ejecta of the Homunculus nebula (Weis, Duschl, & Bomans 2001), which was created after the last great eruption. For HD 5980, however, the ejecta from the 1994 eruption has not had sufficient time to form a detectable LBV nebula around the star, and no 'Homunculus-like' nebula from a previous eruption is visible around HD 5980 (see Fig. 2): any X-ray emission from the colliding ejecta should thus still be blended with the stellar emission from HD 5980 and that may contribute to explain the high X-ray luminosity. Unfortunately, no X-ray detection of HD 5980 before the 1994 eruption is available. A ROSAT all-sky survey image

taken in 1990 (exposure number 933001) provides only an upper limit of $L_X \sim 10^{36}$ erg s^{-1} at the position of HD 5980. Wang & Wu (1992) gave a 3σ upper limit of 2×10^{34} erg s^{-1} for all SMC WR stars, except AB7. These limits are compatible with the detected luminosity of HD 5980 and do not allow us to quantitatively compare the pre- and post-eruption luminosities to confirm the predicted luminosity enhancement.

The fact that HD 5980 is a close binary system containing two very massive stars, suggests that colliding winds may provide another source for the observed X-rays. We can thus estimate the expected X-ray luminosity. For the system, we assume that the stellar winds of the stars have returned to their pre-eruption values and we assume that $\dot{M}_A$=1.4$\times$ 10^{-5} M$_\odot$ yr^{-1}, $v_\infty(A)$=2500 km s^{-1} for the O-star, and $\dot{M}_B$= 2$\times10^{-5}$ M$_\odot$ yr^{-1}, $v_\infty(B)$=1700 km s^{-1} for the WN Wolf-Rayet star (Moffat et al. 1998). Thus the momenta of each star's wind are very similar, and the total wind kinetic energy is 5×10^{37} erg s^{-1}. These wind parameters lead to a momentum ratio of $\eta = (M_B v_\infty(B))/(M_A v_\infty(A)) = 0.97$ (Usov 1992) and the wind-wind collision shock will lie halfway between the stars. In this configuration we expect about 1/6 of the wind kinetic energy to pass perpendicularly through the two shocks and be thermalised (Stevens, Blondin, & Pollock 1992), and because the systems are relatively close much of this energy will be radiated[5].

Consequently, we would expect the X-ray luminosity of HD 5980 to be $\sim 10^{36}$ erg s^{-1} or more, rather than the observed value of $\sim 10^{34}$ erg s^{-1}. The discrepancy between the predicted and observed X-ray luminosities could be due to a range of factors, e.g. the winds may not be at the pre-eruption levels - lower mass-loss rates or lower wind velocities will translate to a lower X-ray luminosity. Radiative braking, wind clumping, or the eclipse of the colliding wind region by the thick wind of star B could also reduce the luminosity. Alternatively, the wind momenta may not be so nearly equal, as a low value of η also tends to lower the luminosity.

Using the ephemeris of Sterken & Breysacher (1997), we have computed a phase of $\phi = 0.24 - 0.30$ for our *Chandra* observation: this is close to the eclipse of star A by star B (ϕ_{ecl}=0.36). If the eccentricity is $e \sim 0.3$, a simple adiabatic model predicts that the X-ray luminosity will vary inversely with separation. We may expect a change in the intrinsic X-ray luminosity of a factor of ~ 2 through the orbit and by $\sim 10\%$ during the *Chandra* observation.

---

[5]In terms of the cooling parameter χ defined by Stevens, Blondin, & Pollock (1992), for the WN wind $\chi \ll 1$ and for the O-star wind $\chi \sim 1$.

We have detected a variation of apparently larger amplitude (factor ∼2) in the count rate of HD 5980 (see Fig. 5b). This still suggests we are seeing orbital variability associated with colliding winds, since the additional effects of changing absorption[6] on the observed luminosity can either reduce or enhance this variability. This observed variability is much more likely to be due to colliding winds than wind-blown bubble type emission, where no short timescale variability would be expected. The high fitted temperature of HD 5980 $kT \sim 7$ keV also suggests that we are likely seeing colliding wind emission, as this temperature corresponds to a shock velocity of ~ 2500 km s^{-1}, comparable to the wind speed of star A ($v_\infty(A)$ above).

The detailed characteristics of the X-ray properties of HD 5980 need to be studied further, in conjunction with detailed colliding wind models (c.f. the case of η Carinae; Pittard & Corcoran 2002). An *XMM-Newton* observation is scheduled at phases $\phi = 0.09 - 0.10$, just after periastron: the comparison between these two datasets may enable us to detect further the signature of the colliding wind region, and constrain it more precisely.

Finally, we note that the unabsorbed X-ray luminosity of the central source in η Carinae, if we assume a distance of 2.3 kpc, varies between (0.6 and 2.5)$\times 10^{35}$ erg s^{-1} (Ishibashi et al. 1999). Such luminosities are much higher than for HD 5980.

5. The Extended Emission around HD 5980

Around the position of HD 5980 lies a region of bright extended X-ray emission. It was first detected by the *Einstein Observatory* (source IKT 18 in Inoue, Koyama, & Tanaka 1983), and subsequently observed by *ROSAT* (source [HFP2000] 148[7] in Haberl et al. 2000). The *Chandra* image reveals the extended emission in much more detail than previous X-ray observatories. The overall shape of the emission region is more or less rectangular, with an extension to the northeast. It contains a few bright or dark arcs, but apart from these, the brightness is rather uniform, with no obvious limb-brightening. It has a size of $130'' \times 100''$, i.e. 37pc×29pc at the SMC's distance. HD 5980 lies towards the top center of the emission region. An X-ray bright filament extends from $9''$ west to $23''$ south of HD 5980. An X-ray dark feature appears some $30''$ at the southeast of HD 5980. The total count rate of this source in the $0.3 - 10.0$ keV energy range is $7.25 \pm 0.17 \times 10^{-2}$ cnts s^{-1}. It is the softest

[6]The colliding wind region is viewed alternatively through the atmosphere of stars A and B. The absorption thus changes with the orbital phase.

[7]This *ROSAT* source may encompass some of the X-ray emission from the cluster.

source present in the field.

The spectrum of this extended X-ray emission was extracted in a rectangular aperture of $\sim 160'' \times 110''$ with a carefully chosen background region, located as close as possible to the source and in a region on the ACIS-I1 CCD where there are no point sources. A circular region of diameter $\sim 5''$ containing HD 5980 was removed from the extraction. As the X-ray emission is extended the reponse matrices were calculated using the *calcrmf* and *calcarf* tools. The best fit (χ^2_ν=1.03, N_{dof}=244) to this spectrum was an absorbed *mekal* model with the following properties (see Fig. 6): $N(H) = 0.12^{0.15}_{0.10} \times 10^{22}$ cm^{-2}, $kT = 0.66^{0.68}_{0.64}$ keV and $Z = 0.17^{0.21}_{0.15} Z_\odot$. The observed flux in the $0.3 - 10.0$ keV band was 3.35×10^{-13} erg cm $^{-2}$ s^{-1}, i.e. an observed luminosity of 1.40×10^{35} erg s^{-1}. The low value of the absorption column, compared to HD 5980 and the cluster, suggests that this X-ray source lies between NGC 346 and the observer, but still in the SMC (see paper II).

Using the normalisation factor of the *mekal* model, we found a volume emission measure $\int n_e n_H dV$ of $\sim 3 \times 10^{58}$ cm^{-3}. Considering a constant density for the hot gas, a sperical geometry of diameter $\sim$33 pc for the extended emission and assuming a pure H composition, the density of the hot gas is roughly 0.2 cm^{-3} and the total mass of the hot gas is $\sim$100 M$_\odot$.

Using the available data, a deeper analysis was conducted, searching for the existence of a temperature gradient throughout the source area, with color and temperature maps. For color maps, we generated a set of narrow-band images, e.g. $0.3 - 0.9$ keV, $0.9 - 1.2$ keV and $1.2 - 2.0$ keV, that enable us to distinguish the harder components from the softer parts. In addition, temperature maps were constructed from spectral fits in small regions of the SNR. The only obvious trend in both the color and temperature maps is the softness of the northeastern extension of the SNR. However, it is not possible to draw any firm conclusions regarding the presence of any temperature gradient.

We have also constructed images of the extended emission in narrow energy bands, each correspond to a specific ion. The energy bands used for each ion are shown in Fig. 7. The data in each band were binned to obtain $4.9'' \times 4.9''$ pixels (see Fig. 7). In contrast to N132D (Behar et al. 2001), no significative differences between the morphology of highly ionized species (Mg^{10+}, Ne^{9+}, Si^{12+}, Fe^{19+}) and lower ionization species were detected.

5.1. The Nature of the Extended Emission

Since its discovery the extended X-ray emission has been attributed to a supernova remnant (SNR). Further evidence was subsequently obtained to support this hypothesis; for example, Ye, Turtle, & Kennicutt (1991) found a non-thermal radio source at this position that they called SNR 0057 − 7226. Using the lowest contours of Ye, Turtle, & Kennicutt (1991), the radio source is 56 pc×52 pc, slightly larger than the X-ray source.

Moreover, evidence of high velocity motions in this region were observed in the visible and UV ranges. Using echelle spectra centered on Hα, Chu & Kennicutt (1988) found clumps moving at $v_{LSR} \sim 300\,km\,s^{-1}$, redshifted from the main quiescent component by $+170\,km\,s^{-1}$: only the receding side of the expanding object is seen, suggesting a low density where the approaching side arises. UV analyses with *IUE* (de Boer & Savage 1980), *HST* STIS (Koenigsberger et al. 2001) and *FUSE* (Hoopes et al. 2001) have also confirmed the presence of an expanding structure. While de Boer & Savage (1980) and Hoopes et al. (2001) found only absorptions at v_{LSR}=+300 km s^{-1}, Koenigsberger et al. (2001) detected both expanding sides of the object, with components at $v_{LSR} = +21, +52, +300, +331\,km\,s^{-1}$. However, the absorptions at +21 and +52 km s^{-1} were small, and need a future confirmation. The presence of components from both approaching and receding sides of the expanding structure has now been confirmed by Danforth et al. (2002) from deep echelle spectroscopic integrations at optical wavelengths of the N66 region. Absorptions at any of these velocities are not seen in the spectra of Sk 80, a close neighbor of HD 5980 situated on the edge of the X-ray source. A fast expanding structure close to the position of HD 5980 is thus present.

Unfortunately, even the high-resolution *HST* WFPC2 images of the close neighborhood of HD 5980 do not show any clear nebula associated with the X-ray extended emission (see Fig. 2). A lot of filamentary structures - generally indicative of a SNR (Chen et al. 2000) - are seen throughout the field, but are not limited to the exact location of the X-ray source. There is thus no obvious Hα feature directly correlated with the extended X-ray emission.

Considering all the evidence (non-thermal emission, high velocity expanding shell etc), the X-ray / radio source should thus be regarded as a SNR located in front of HD 5980 but still belonging to the SMC. The SNR hypothesis is further supported by the comparison of the size of this feature to its X-ray and radio fluxes (Mathewson et al. 1983).

As HD 5980 is projected more or less at the center of the diffuse X-ray emission and

it underwent a LBV-type eruption in 1994 (which is unlikely to be the only one undergone by the system), it is tempting to associate the diffuse X-ray emission with HD 5980. To investigate whether this association is likely, we first compare HD 5980 with η Carinae, the most well-known LBV that have gone through multiple eruptions. η Car is also surrounded by bright, extended X-ray emission that appears to be assciated with the Carina Nebula: it is comparable in X-ray temperature (kT), size and morphology to the X-ray emission around HD 5980 (Seward & Mitchell 1981; Fig.8). But it is generally assumed that this Nebula has been formed through the collective action of all stars of the Carina cluster, not only by the single action of η Carinae.

We have also searched for clues of an interaction between HD 5980 and its surroundings (e.g. a LBV nebula). Walborn (1978) noted evidence of such interaction: an arc of radius $\sim 30''$ centered on the star is actually visible in Hα and [O III] (but not in [S II]). However, this arc is rather diffuse (see Fig. 2), indicating a lack of shock compression. Moreover, its velocity coincides with that of the quiescent region, and no line-splitting region is seen beginning at the arc and extending towards the star (Danforth et al. 2002): this arc is certainly not the rim of an expanding shell. This optical arc has different size, shape, and location from an X-ray bright arc (Fig. 2), therefore we conclude that they are probably two distinct features unrelated to each other. Echelle spectra of this area also do not show any enhancement of the [N II]/Hα ratio which usually indicates the presence of circumstellar material surrounding the star. The comparison between X-rays and visible data thus do not show any clear indication of an interaction between HD 5980 and its environment. We also note that no circumstellar nebula produced by HD 5980 could explain the redshifted UV absorptions in the spectra of the star, or the non-thermal radio emission from the extended source.

The last possibility is that the source is indeed a SNR, but that HD 5980 is still directly responsible for it. Several authors have proposed the existence of a third component in HD 5980, 'star C', to interpret the visual light curve (Breysacher & Perrier 1991) and the presence of stable photospheric absorptions in UV (Koenigsberger et al. 2000). To explain the existence of a SNR, an additional, fourth component of the system, 'star D', is needed. It would now be a compact object, a remnant of the star that exploded in SN long ago. If star C is much farther away than the system A+B+D, then the high velocity redshifted UV absorptions could be produced by star C shining through the receding back wall of the SNR. The presence of a compact object might explain the $\sim$6 h variations seen in the lightcurve of HD 5980 by Sterken & Breysacher (1997). Accretion onto this compact object might also constitute another source of X-rays, thus contributing to understand the high X-ray emission

from the system.

6. Summary

In this series of articles, we report the analysis of the *Chandra* data of N66, the largest star formation region of the SMC. In this first paper, we have focused on the most important objects of the field: the NGC 346 cluster and HD 5980.

The cluster itself is relatively faint, with a total luminosity of $L_X^{unabs} \sim 1.5 \times 10^{34}$ erg s^{-1} in the 0.3-10.0 keV energy range. Most of this emission seems correlated with the location of the brightest stars of the core of the cluster, but the level of X-ray emission probably cannot be explained solely by the emission from individual stars.

In this field lies another object of interest: HD 5980, a remarkable star that underwent a LBV-type eruption in 1994. *Chandra* is in fact the first X-ray telescope to detect HD 5980 individually. In X-rays, the star appears very bright, comparable only to the brightest WR stars in the Galaxy, but still fainter than η Carinae. The comparison of our results with future X-ray observations will enable us to better understand HD 5980: for example, phase-locked variations will be analysed in the perspective of the colliding wind behaviour of this binary, while other variations may be related to the recent LBV eruption. Follow-up observations are thus needed to complete the study of this system.

A bright, extended X-ray emission is seen to surround HD 5980. It is most probably due to a SNR whose progenitor is unknown. The spatial coincidence of this extended X-ray emission with the peculiar massive star suggest an association between these two objects. We also note the close resemblance of this X-ray emission to the Carina Nebula in which the LBV η Carinae lies.

We are grateful to Dr Martin A. Guerrero Roncel for useful suggestions on data analysis techniques. Support for this work was provided by the National Aeronautics and Space Administration through Chandra Award Number GO1-2013Z issued by the Chandra X-Ray Observatory Center, which is operated by the Smithsonian Astrophysical Observatory for and on behalf of NASA under contract NAS8-39073. Y.N. acknowledges support from the

PRODEX XMM-OM and Integral Projects, contracts P4/05 and P5/36 'Pôle d'attraction Interuniversitaire (SSTC-Belgium) and from PPARC for an extended visit to the University of Birmingham. IRS and JMH also acknowledge support from PPARC. AFJM thanks NSERC (Canada) and FCAR (Quebec) for financial aid. This research has made use of the SIMBAD databse, operated at CDS, Strasbourg, France and NASA's Astrophysics Data System Abstract Service.

REFERENCES

Arnaud, K. 1996, ASP Conf. Ser. 101, eds G. Jacoby & J. Barnes, p.17

Behar, E., Rasmussen, A.P., Griffiths, R.G., Dennerl, K., Audard, M., Aschenbach, B., & Brinkman, A.C. 2001, A&A, 365, L242

Berghöfer, T.W., Schmitt, J.H.M.M., Danner, R., & Cassinelli, J.P. 1997, A&A, 322, 167

Breysacher, J. & Perrier, C. 1991, IAUS 143, 229

Cantó, J., Raga, A.C., & Rodríguez, L.F. 2000, ApJ, 536, 896

Chen, C.-H. R., Chu, Y.-H., Gruendl, R.A., & Points, S.D. 2000, AJ, 119, 1317

Chu, Y.-H., & Kennicutt, R.C., Jr 1988, AJ, 95, 1111

Danforth et al., 2002, in preparation

de Boer, K.S., & Savage, B.D. 1980, ApJ, 238, 86

Getman, K.V., Feigelson, E.D., Townsley, L., Bally, J., Lada, C.J., & Reipurth B. 2002, to be published in ApJ, 575

Haberl, F., Filipovic, M. D., Pietsch, W., & Kahabka, P. 2000, A&AS, 142, 41 (HFP2000)

Haberl, F., & Sasaki, M. 2000, A&A 359, 573

Henize, K.G. 1956, ApJS, 2, 315

Hoopes, C.G., Sembach, K.R., Howk, J.C., & Blair, W.P. 2001, ApJ, 558, L35

Humphreys, R.M. & McElroy, D.B. 1984, ApJ, 284, 565

Inoue, H., Koyama, K., & Tanaka, Y. 1983, IAUS 101, 535 (IKT)

Ishibashi, K., Corcoran, M.F., Davidson, K., Swank, J.H., Petre, R., Drake, S.A., Damineli, A., & White, S. 1999, ApJ, 524, 983

Kaastra, J.S. 1992, An X-Ray Spectral Code for Optically Thin Plasmas (Internal SRON-Leiden Report, updated version 2.0)

Kahabka, P., Pietsch, W., Filipovic, M. D., & Haberl, F. 1999, A&AS, 136, 81

Koenigsberger, G., Georgiev, L., Barbà, R., Tzvetanov, Z., Walborn, N.R., Niemela, V.S., Morrell, N., & Schulte-Ladbeck, R. 2000, ApJ, 542, 428

Koenigsberger, G., Georgiev, L., Peimbert, M., Walborn, N.R., Barbà, R., Niemela, V.S., Morrell, N., Tsvetanov, Z., & Schulte-Ladbeck, R. 2001, AJ, 121, 267

Massey, P., Parker, J.W., & Garmany, C.D. 1989, AJ, 98, 1305

Mathewson, D.S., Ford, V.L., Dopita, M.,A., Tuohy, I.R., Long, K.S., & Helfand, D.J. 1983, ApJS, 51, 345

Mathewson, D.S., Ford, V.L., & Visvanathan, N. 1986, ApJ 301, 664

Moffat, A.F.J., Marchenko, S.V., Bartzakos, P., Niemela, V.S., Cerruti, M.A., Magalhaes, A.M., Balona, L., St-Louis, N., Seggewiss, W., & Lamontagne, R. 1998, ApJ, 497, 896

Moffat, A.F.J., et al., 2002, ApJ, (in press)

Nazé et al., in preparation (paper II)

Ozernoy, L.M., Genzel, R., & Usov, V.V. 1997, MNRAS, 288, 237

Pittard, J.M., & Corcoran, M.F. 2002, A&A, 383, 636

Pollock, A.M.T. 2002, Interacting winds from massive stars, eds A.F.J. Moffat & N. St Louis, ASP Conf. Series, 260, p 363

Puls, J., Kudritzki, R.-P., Herrero, A., Pauldrach, A.W.A., Haser, S.M., Lennon, D.J., Gabler, R., Voels, S.A., Vilchez, J.M., Wachter, S., & Feldmeier, A. 1996, A&A, 305, 171

Raga, A.C., Velázquez, P.F., Cantó, J., Masciadri, E., & Rodríguez, L.F. 2001, ApJ, 559, L33

Sasaki, M., Haberl, F., & Pietsch, W. 2000, A&AS, 147, 75

Schmidtke, P.C., Cowley, A.P., Crane, J.D., Taylor, V.A., McGrath, T.K., Hutchings, J.B., & Crampton, D. 1999, AJ, 117, 927

Seward, F.D. & Mitchell, M. 1981, ApJ, 243, 736

Seward, F.D., Butt, Y.M., Karovska, M., Prestwich, A., Schlegel, E.M., & Corcoran, M. 2001, ApJ, 553, 832

Sterken, C. & Breysacher, J. 1997, A&A, 328, 269

Stevens I.R., Blondin J.M., Pollock, A.M.T. 1992, ApJ, 386, 265

Townsley, L.K., Broos, P.S., Garmire, G.P., & Nousek, J.A. 2000, ApJ, 534, L139

Usov, V.V. 1992, ApJ, 389, 635

Walborn, N.R. 1978, ApJ, 224, L133

Walborn, N.R., Howarth, I.D., Lennon, D.J., Massey, P., Oey, M.S., Moffat, A.F.J., Skalkowski, G., Morrell, N.I., Drissen, L., & Parker, J.W. 2002, AJ, 123, 2754

Wang, Q. & Wu, X. 1992 ApJS, 78, 391

Weis, K., Duschl, W.J., & Bomans, D.J. 2001, A&A, 367, 566

Wessolowski, U. 1996, MPE report No. 263, 75

Ye, T., Turtle, A.J., & Kennicutt, R.C., Jr. 1991, MNRAS, 249, 722

Yokogawa, J., Imanishi, K., Tsujimoto, M., Nishiuchi, M., Koyama, K., Nagase, F., & Corbet, R.H.D. 2000, ApJS, 128, 491

Yusef-Zadeh, F., Law, C., Wardle, W., Wang, Q.D., Fruscione, A., Lang, C.C., Cotera A. 2002, ApJ, 570, 665

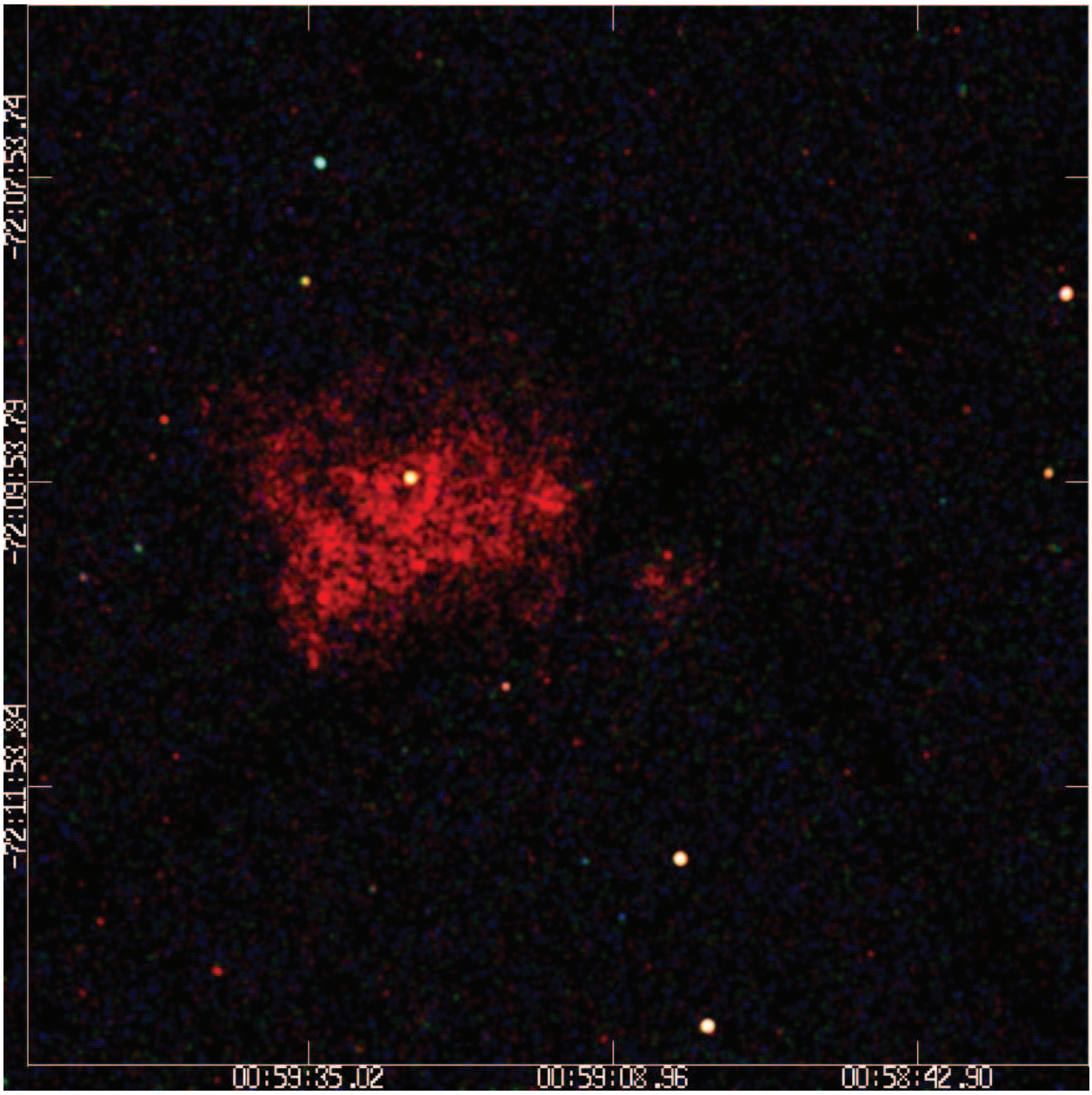

Fig. 1.— *Chandra* color image of the region close to HD 5980. Three energy bands were used to create this color image : red corresponds to 0.3-1.0 keV, green to 1.0-2.0 keV and blue to 2.0-10.0 keV. Before combination, the images were smoothed by convolution with a gaussian of σ=1″.

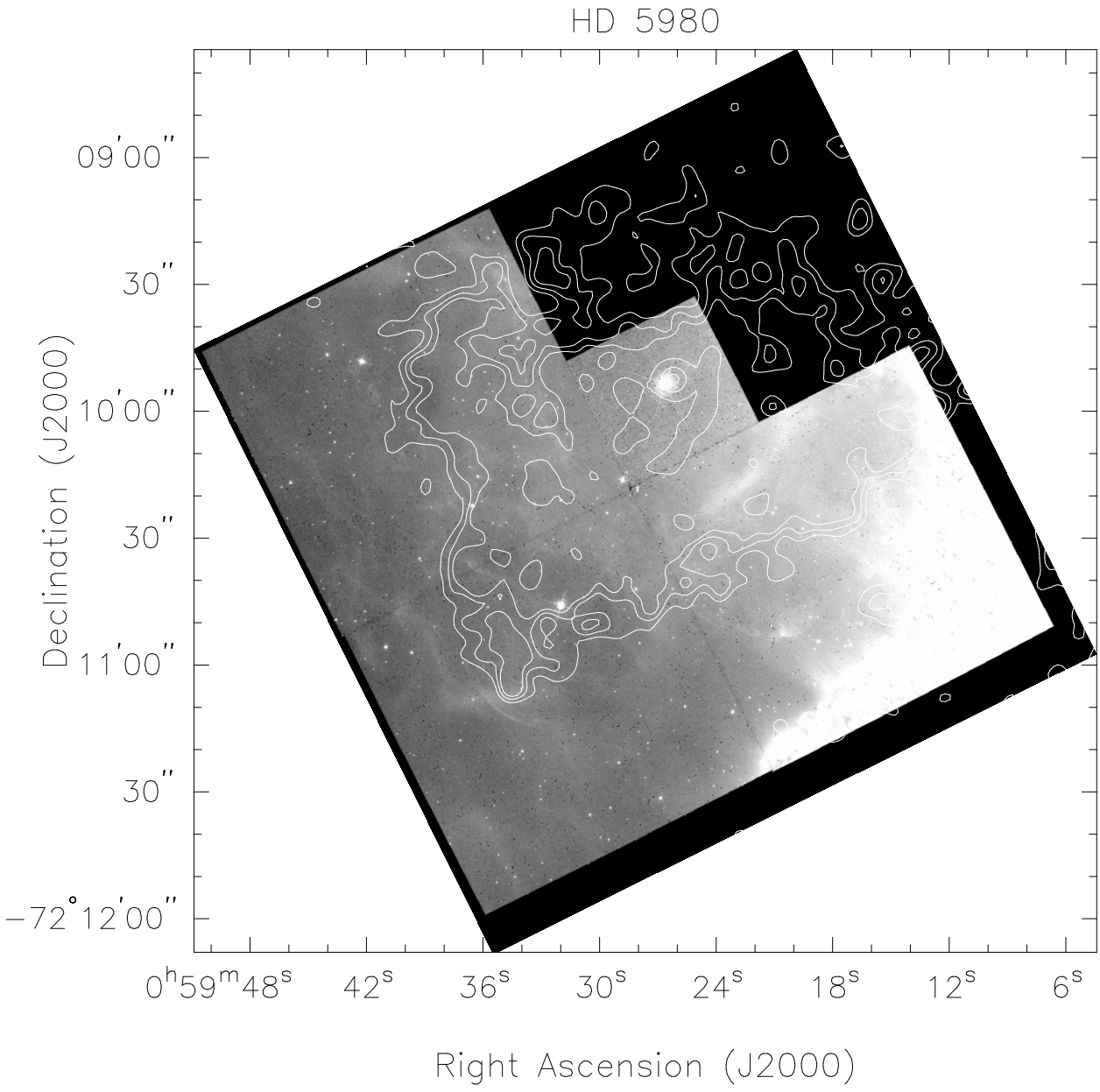

Fig. 2.— *HST* WFPC2 Hα data of the region surrounding HD 5980 (which is the star located at the center of the PC chip). The X-ray data overlaid as contours on the *HST* image were first binned by a factor of 2 and then smoothed by convolution with a gaussian of σ=2″.

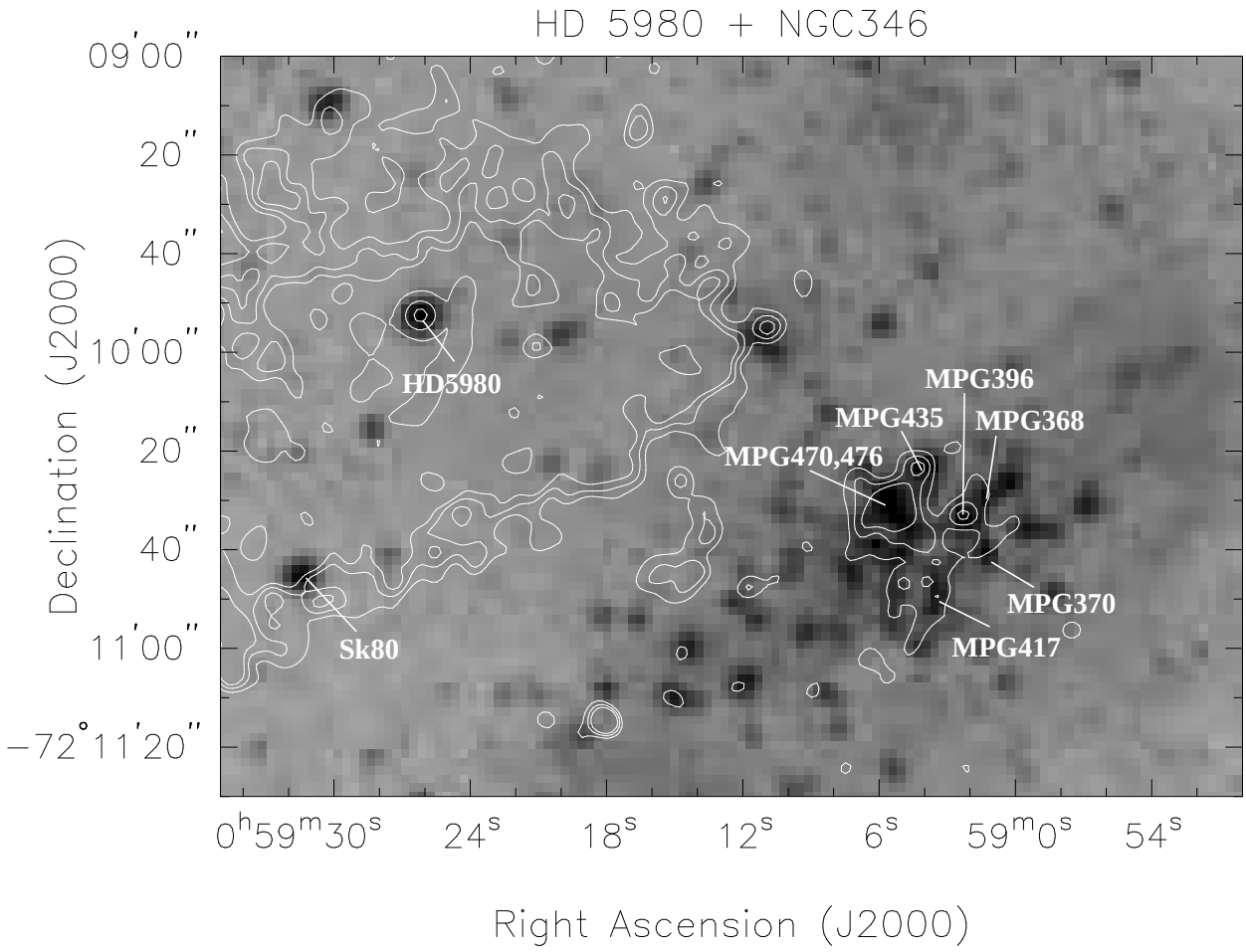

Fig. 3.— The *Chandra* X-ray data of the NGC 346/HD 5980 region superimposed on the *DSS* image, showing the extended nature of the X-ray source associated with the cluster. The location of the brightest stars in the cluster are indicated. The X-ray data were first binned by a factor of 2 and then smoothed by convolution with a gaussian of $\sigma = 2''$)

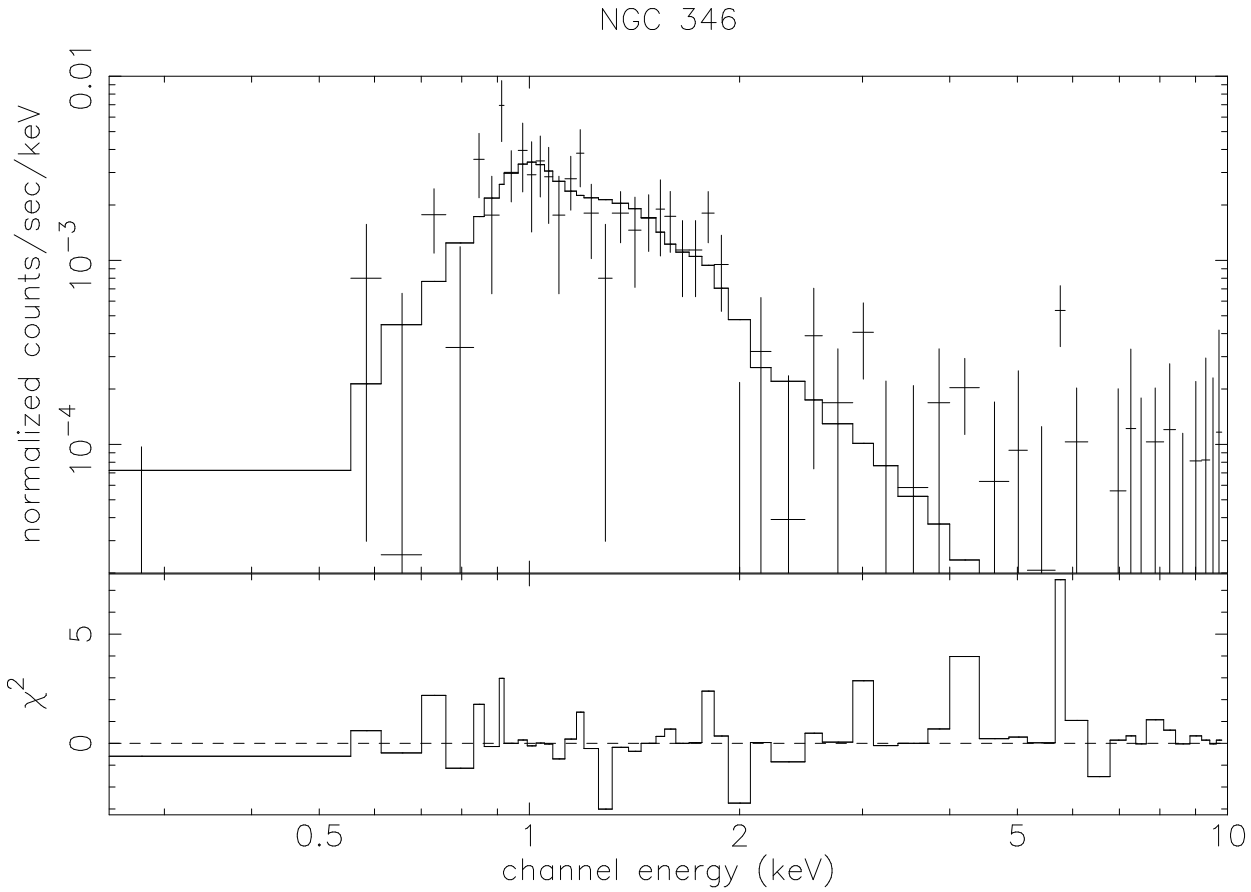

Fig. 4.— The X-ray spectrum of the NGC 346 cluster, shown along with the best-fit absorbed *mekal* model, with $N(H) = 0.42 \times 10^{22}$ cm^{-2} and $kT = 1.01$ keV (see § 3).

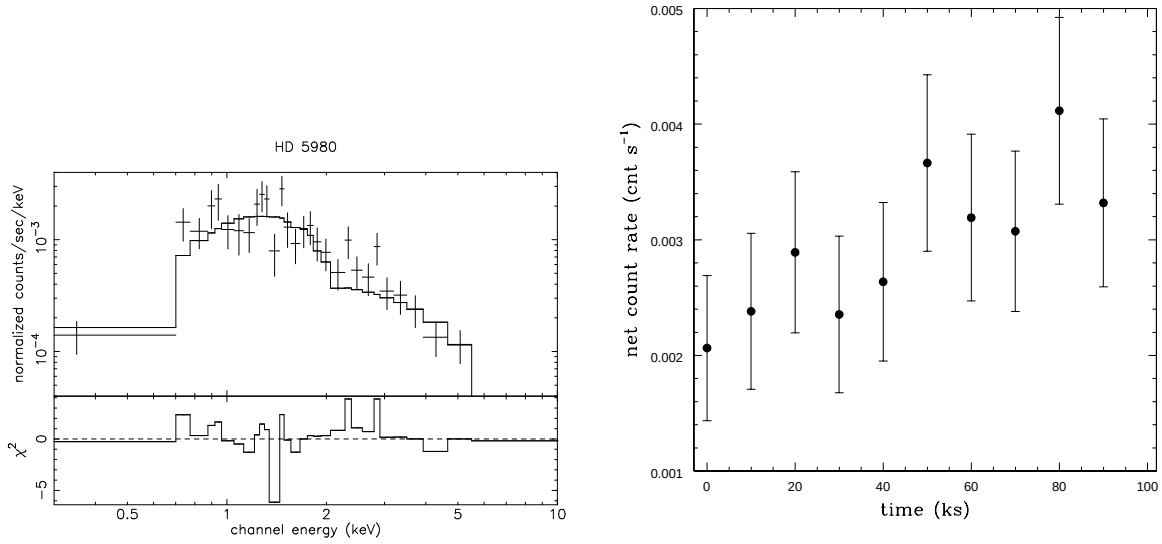

Fig. 5.— a. The *Chandra* X-ray spectrum of HD 5980, shown along with the best-fit absorbed *mekal* model, with $N(H) = 0.22 \times 10^{22}$ cm^{-2} and $kT = 7.04$ keV. b. The *Chandra* X-ray lightcurve of HD 5980, in the 0.3-10 keV range and with 10 bins of 10 ks each.

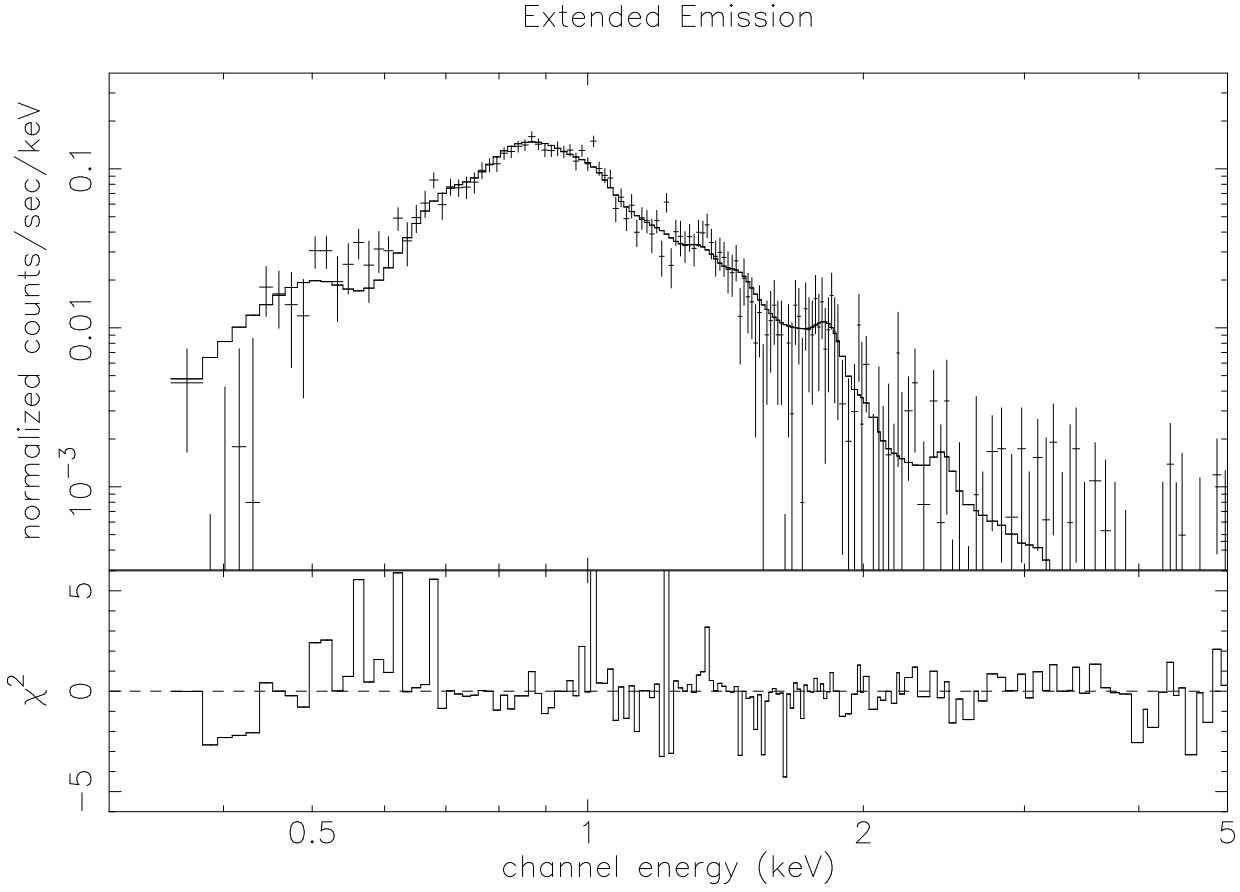

Fig. 6.— The *Chandra* X-ray spectrum of the extended emission around HD 5980, shown along with the best-fit absorbed *mekal* model, with $N(H) = 0.12 \times 10^{22}$ cm^{-2}, $kT = 0.66$ keV and $Z = 0.17 Z_{\odot}$ (see § 5).

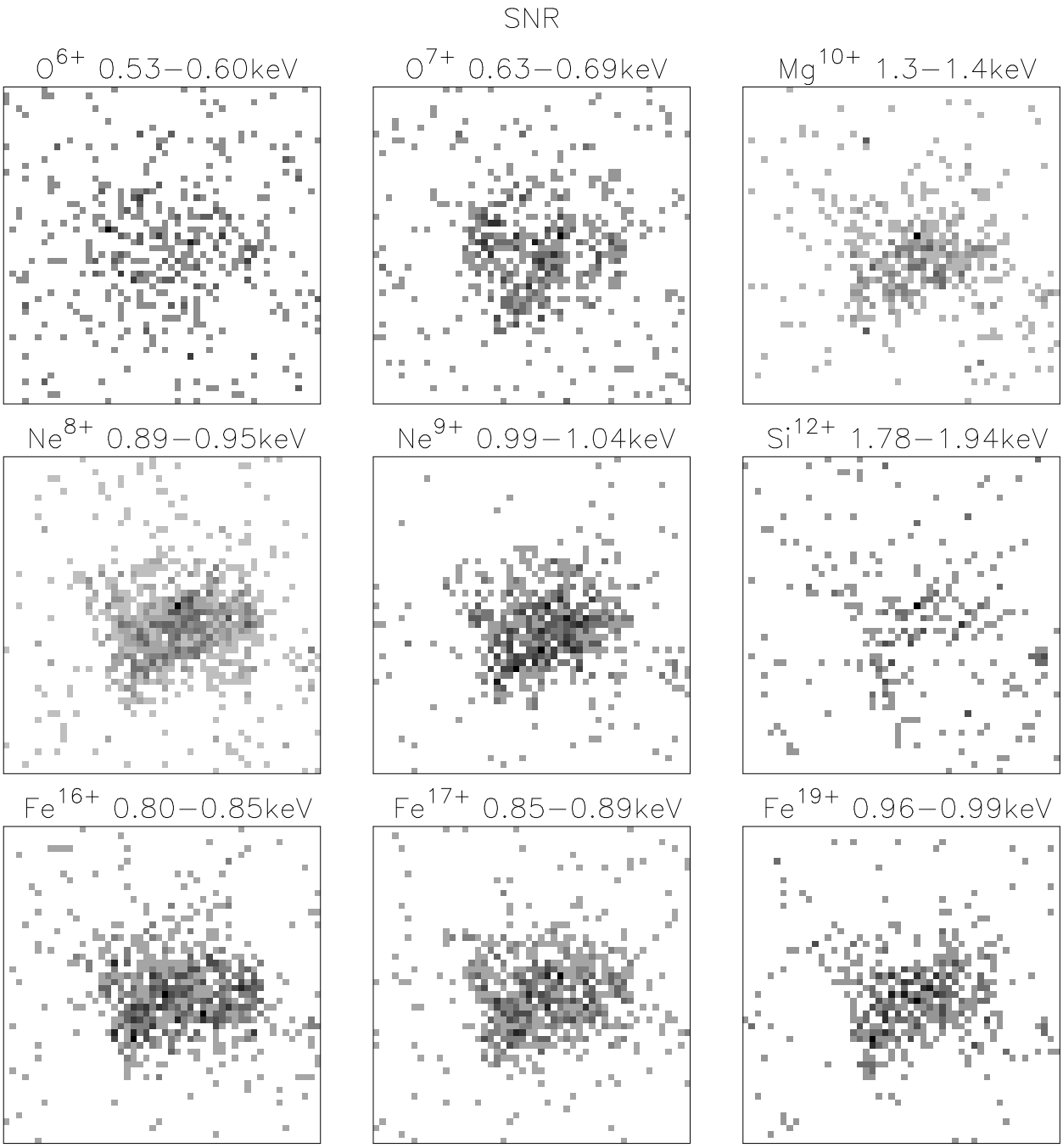

Fig. 7.— Narrow-band X-ray images of the extended emission surrounding HD 5980. Each image is labeled with the principal line-emitting ion and the energy range used to generate the image.

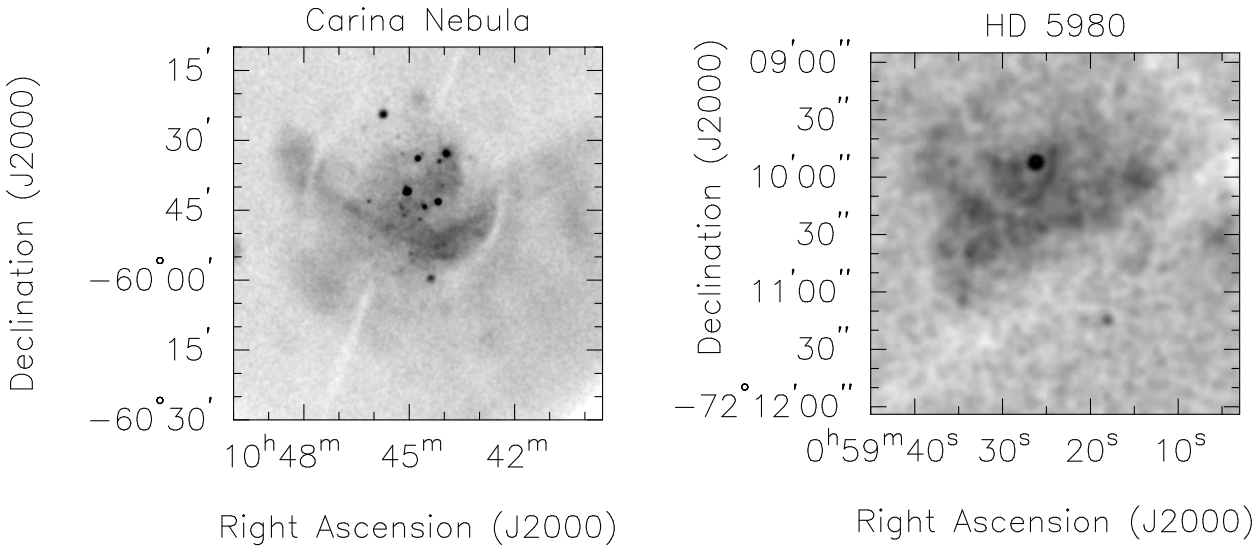

Fig. 8.— X-ray images of the Carina Nebula (24 ks ; ROSAT PSPC observation #900176) compared to the extended emission around HD 5980. If we assume a distance of 2.3 kpc for the Carina Nebula and 59 kpc for the SMC, both images are ∼55 pc×55 pc. ROSAT PSPC support rings and *Chandra* ACIS-I CCD gaps can be spotted on these images. Both images were smoothed by convolution with a gaussian (σ=15″ for the Carina Nebula and σ=2″ after binning by a factor of 2 for HD 5980).